JEM Journal of Experimental Medicine

BRIEF DEFINITIVE REPORT

# CD150-dependent hematopoietic stem cell sensing of *Brucella* instructs myeloid commitment

Lisiena Hysenaj[1,2], Bérengère de Laval[1], Vilma Arce-Gorvel[1], Mile Bosilkovski[3], Gabriela González-Espinoza[1], Guilhaume Debroas[1], Michael H. Sieweke[1,4], Sandrine Sarrazin[1], and Jean-Pierre Gorvel[1]

**So far, hematopoietic stem cells (HSC) are considered the source of mature immune cells, the latter being the only ones capable of mounting an immune response. Recent evidence shows HSC can also directly sense cytokines released upon infection/inflammation and pathogen-associated molecular pattern interaction while keeping a long-term memory of previously encountered signals. Direct sensing of danger signals by HSC induces early myeloid commitment, increases myeloid effector cell numbers, and contributes to an efficient immune response. Here, by using specific genetic tools on both the host and pathogen sides, we show that HSC can directly sense *B. abortus* pathogenic bacteria within the bone marrow via the interaction of the cell surface protein CD150 with the bacterial outer membrane protein Omp25, inducing efficient functional commitment of HSC to the myeloid lineage. This is the first demonstration of direct recognition of a live pathogen by HSC via CD150, which attests to a very early contribution of HSC to immune response.**

## Introduction

Few pathogens are capable of colonizing the bone marrow (BM; Nebe et al., 2005; Eldin et al., 2016; Allen et al., 2014; Hardy et al., 2009; Reece et al., 2018), the niche of hematopoietic stem cells (HSC) responsible for initiating the production of myeloid progenitors and mature blood-forming cells (Weissman, 2014). *Brucella abortus* (a Gram-negative bacterium responsible for the re-emerging brucellosis zoonosis) is able to persist for months in the BM (Gutiérrez-Jiménez et al., 2018). Human brucellosis patients suffer from hematological abnormalities, suggesting that *B. abortus* in the BM may affect hematopoietic development (Franco et al., 2007). HSC can respond to infection through pathogen-elicited cytokines or directly via pathogen recognition receptors (Boettcher et al., 2014; Boettcher and Manz, 2017). CD150 is a key marker of long-term HSC (LT-HSC; Kiel et al., 2005). It was originally described on T and B cells as a measles virus receptor (Tatsuo and Yanagi, 2002; Erlenhoefer et al., 2001) and as a bacterial sensor in macrophages (Berger et al., 2010) and dendritic cells (Degos et al., 2020). Here, we show that HSC in the BM directly sense the outer membrane protein Omp25 of *B. abortus* through the CD150 receptor. Our in vivo and ex vivo data demonstrate that *B. abortus* modulates hematopoiesis by transiently increasing the production of myeloid cells via CD150. This is the first demonstration of direct recognition of a pathogen by HSC via CD150.

## Results and discussion

### *B. abortus* persists in the BM and is transferable to a second host but does not infect HSC

We investigated the consequences of BM infection by a pathogen such as *B. abortus* that we previously demonstrated to persist for months in the hematopoietic niche (Gutiérrez-Jiménez et al., 2018). We first evaluated if bacteria present in the BM 8 d after infection during the acute phase of infection and 30 d after infection during the chronic phase of infection are still virulent and transferable to a secondary host. For this, we transplanted BM cells of infected mice at these time points into recipient mice (Fig. S1 a) and enumerated CFU in splenocytes and BM cells 8 wk after transplantation (Fig. S1 b). An equivalent high number of CFU counts in the spleen and the BM 8 wk after transplantation showed that following BM transplantation, the host BM hematopoietic environment is permissive for stable infection and replication of *B. abortus* as it is in the spleen, the natural reservoir for *B. abortus* in mice.

[1]Aix Marseille University, Centre National de la Recherche Scientifique, Institut National de la Santé et de la Recherche Médicale, Centre d'Immunologie de Marseille-Luminy, Marseille, France; [2]Department of Anatomy, University of California, San Francisco, San Francisco, CA, USA; [3]University Clinic for Infectious Diseases and Febrile Conditions, Skopje, Republic of North Macedonia; [4]Center for Regenerative Therapies Dresden, Technische Universität Dresden, Dresden, Germany.

Correspondence to Sandrine Sarrazin: sarrazin@ciml.univ-mrs.fr; Jean-Pierre Gorvel: gorvel@ciml.univ-mrs.fr

L. Hysenaj and B. de Laval are co-first authors. M.H. Sieweke, S. Sarrazin, and J.P. Gorvel are co-last authors.

Since in mature lymphoid and myeloid cells CD150 has been shown to be a receptor for cellular entry of viruses and a sensor of bacteria, including *B. abortus* (Tatsuo and Yanagi, 2002; Erlenhoefer et al., 2001), and since CD150 is highly expressed and a commonly used marker of HSC but has no assigned function in these cells (Kiel et al., 2005), we speculated that *B. abortus* might infect HSC via CD150. We therefore isolated HSC and several downstream progenitor populations from the BM of wt mice, incubated them for 2 h in the presence of live *B. abortus*, washed off bacteria, and enumerated bacterial CFU counts of lysed cells 24 h later. Surprisingly, only granulocyte–monocyte progenitors (GMP), but not HSC or multipotent progenitors, were able to support *B. abortus* replication (Fig. 1 a). Since GMP do not express CD150 at their surface (Fig. 1 b), this suggested that CD150 is not required for *B. abortus* entry into the cells. To further confirm this, we incubated wt or *CD150*$^{-/-}$ progenitors (lin$^-$ cells) or HSC with dsRed-labeled *B. abortus* and investigated infection efficiency by confocal microscopy (Fig. 1 c). Although dsRed-*B. abortus* was able to enter both wt and *CD150*$^{-/-}$ lin$^-$ cells, neither wt nor *CD150*$^{-/-}$ HSC were infected (Fig. 1 c). Taken together, these results indicate that CD150 does not play the role of an entry receptor for *B. abortus* in hematopoietic stem or progenitor cells.

### Presence of *B. abortus* in BM affects hematopoietic stem and progenitor cell (HSPC) homeostasis

Given the persistence of *B. abortus* in the hematopoietic niche during the course of infection, we wondered whether the bacterium could affect hematopoietic stem and progenitor cells in ways other than direct infection of HSC. We therefore analyzed the composition of the HSPC compartment after infection by *B. abortus* by flow cytometry. Absolute numbers of total BM cells or lineage negative progenitors (lin$^-$) were not affected by *B. abortus* infection (Fig. S1, c and d). However, *B. abortus* infection induced major phenotypic cell surface marker changes in the HSPC compartment (Fig. 1, d and e; and Fig. S2 for gating strategy), similar to those observed after challenges with pathogen-associated molecular patterns or attenuated vaccines (Boettcher and Manz, 2017; Takizawa et al., 2017; Mitroulis et al., 2018; Kobayashi et al., 2015). HSPC (LSK: lin$^-$, Sca$^+$, cKit$^+$) expansion was observed at the onset of infection (day 2 after infection; Fig. 1, d and e) and was even more pronounced during the acute phase of infection (day 8 after infection; Fig. 1, d and e). LSK expansion was mainly due to the significant increase of CD48$^+$ multipotent progenitors (LSK CD48$^+$) and, to a lesser extent, the increase of short-term HSC (LSK, CD34$^-$, CD135$^-$ CD48$^-$, CD150$^-$; Fig. 1, d and e). In addition, the LT-HSC population (LSK, CD34$^-$, CD135$^-$, CD48$^-$, CD150$^+$) slightly decreased (Fig. 1, d and e). Overall, these data suggest that the presence of *B. abortus* in the BM perturbs HSPC homeostasis and leads to an increased output of early multipotent progenitors.

### *B. abortus* induces PU.1 expression in HSC via a direct Omp25/CD150 recognition

We next investigated the molecular mechanisms underlying the early response of HSC during *B. abortus* infection. HSC can directly sense microbial compounds (Kobayashi et al., 2015; Takizawa et al., 2017; Burberry et al., 2014), and in dendritic cells and macrophages, CD150 is also a sensor for bacteria (Berger et al., 2010; Degos et al., 2020). We therefore speculated that CD150-mediated pathogen sensing might be involved in the observed activation and differentiation of HSC induced by *B. abortus* infection.

To address this question, we used a system that can read out early myeloid lineage engagement of HSC. Infection and inflammation have been shown to release signals such as cytokines that are able to induce the differentiation of HSC toward the myeloid lineage as evidenced by early upregulation of the myeloid master regulator PU.1 (Takizawa et al., 2012; Pronk et al., 2011; Pietras, 2017; Mossadegh-Keller et al., 2013; Sarrazin et al., 2009). Consistent with this, we have previously shown (Sarrazin et al., 2009; Mossadegh-Keller et al., 2013; de Laval et al., 2020) that GFP expression in HSC of *Pu.1*$^{+/GFP}$ reporter mice harboring enhanced GFP knocked into the PU.1 locus (Back et al., 2004; Bryder et al., 2006) is a reliable read-out of early HSC activation and myeloid commitment. To investigate whether *B. abortus* infection can induce an early cell fate change toward the myeloid lineage in HSC, we infected *Pu.1*$^{+/GFP}$ reporter mice and then analyzed GFP expression in HSC (LSK, CD34$^-$, CD135$^-$, CD48$^-$) 2 d after infection (Fig. 2 a). GFP was upregulated 30–40% in BM HSCs of wt mice infected with *B. abortus* WT (Ba WT; Fig. 2 b), confirming induction of PU.1 expression and consequently a change in HSC fate after *B. abortus* infection.

We next analyzed whether this involved a direct interaction of *B. abortus* with CD150. We have recently demonstrated that the outer membrane protein 25 (Omp25) of *B. abortus* is a direct ligand of the extracellular domain of mouse CD150 in dendritic cells (Degos et al., 2020). To analyze whether this direct Omp25/CD150 recognition might be important in HSC, we first analyzed PU.1 expression in HSC during infection with Ba WT and *B. abortus* lacking Omp25 (Ba Δ*omp25*) in *Pu.1*$^{+/GFP}$ reporter mice (Fig. 2 a). 2 d after infection, although CFU counts in the spleen and the BM were similar for both bacterial strains (Fig. S1 e), the upregulation of PU.1 observed in HSC in response to Ba WT infection was abolished in response to Ba Δ*omp25* (Fig. 2 b). The presence of Omp25 at the *B. abortus* membrane is thus required to induce a myeloid HSC commitment.

To further examine whether the presence of CD150 at the HSC surface was also necessary for the recognition of *B. abortus*, we generated a new *Pu.1*$^{+/GFP}$ reporter mouse model lacking CD150 (*CD150*$^{-/-}$*; Pu.1*$^{+/GFP}$). Infected *CD150*$^{-/-}$*; Pu.1*$^{+/GFP}$ mice showed an equivalent bacterial load in both spleen and BM during the onset and acute phase of infection (Fig. S1, e and f). Moreover, the absence of CD150 did not affect either the total number of BM cells or the number of lin$^-$ cells in infected mice (Fig. S1, c and d). 2 d after infection, BM HSC from *CD150*$^{-/-}$*; Pu.1*$^{+/GFP}$ mice did not show any increase of GFP expression, in contrast to what we observed in *Pu.1*$^{+/GFP}$ mice (Fig. 2 b), indicating that the induction of PU.1 by *B. abortus* in HSC requires CD150. These data show that PU.1 upregulation in HSC during the onset of infection is dependent on Omp25/CD150 interaction.

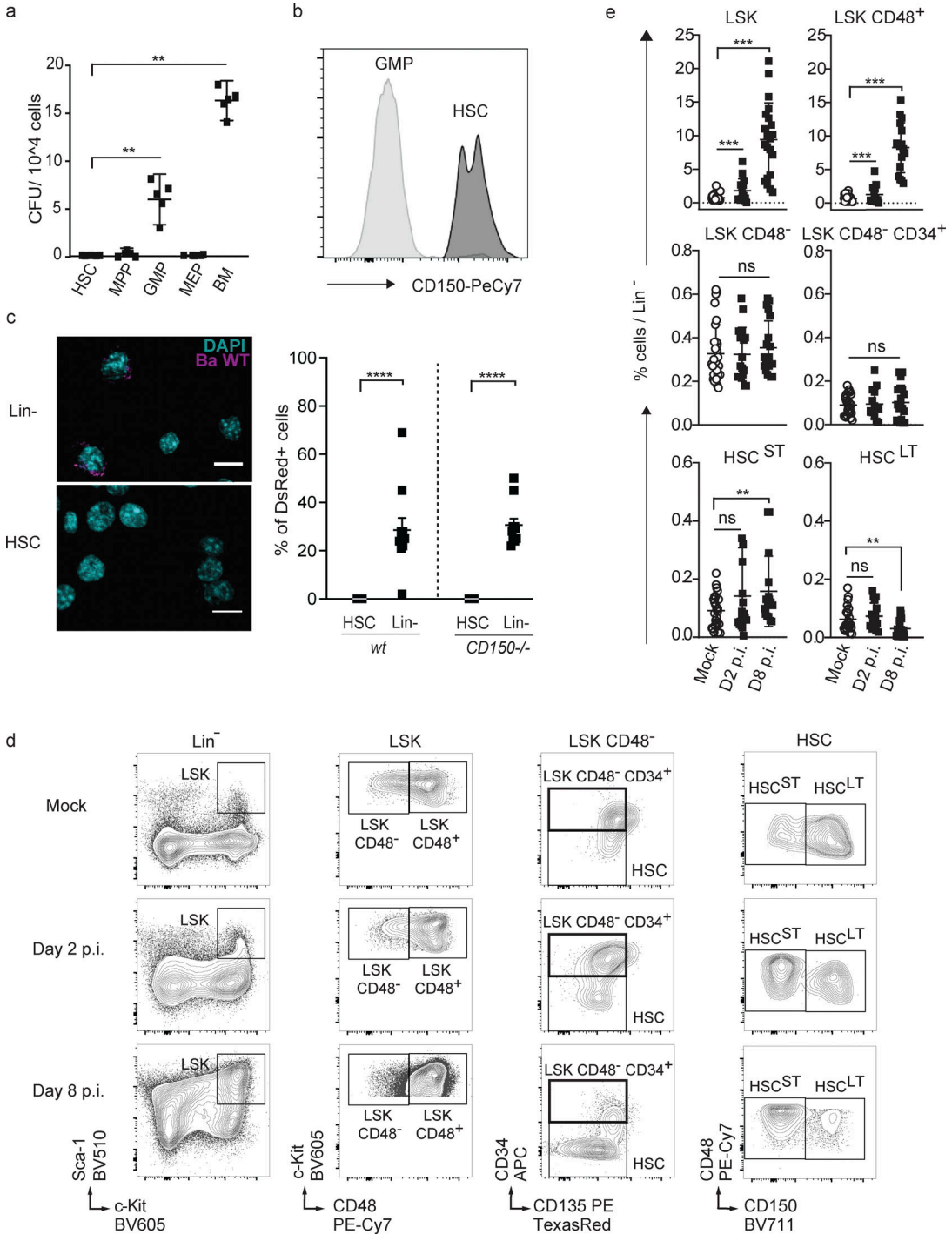


Figure 1. **HSCs are not infected by *B. abortus*, but HSPC homeostasis is affected by the persistence of *B. abortus* in the BM. (a)** Bacterial CFU counts from purified HSC, progenitors (MPP, GMP, MEP), and total BM 24 h after ex vivo infection with *B. abortus*. Data were obtained from distinct samples ($n$ = 5; cells from a pool of two mice in each sample) and from two independent experiments. **(b)** Expression level of CD150 protein on GMP and HSC by FACS. Significant differences from HSC are shown (a and b). **(c)** Identification by confocal microscopy and quantification of wt and *CD150*$^{-/-}$ HSC and BM lin$^-$ cells infected with ds-Red–expressing *B. abortus* 24 h after exposure. Scale bar = 10 µm. Each dot represents the percentage of positive cells in a picture (5–20 cells per slide). Data were obtained from two independent experiments (each cell from a pool of two mice). **, P < 0.01; ****, P < 0.0001; absence of P value, non-significant. P values were generated using Mann–Whitney test. **(d and e)** C57BL/6J wt mice were intraperitoneally inoculated with 1 × 10$^6$ CFU of Ba WT. 2 (D2) and 8 d (D8) later, FACS analyses were performed for BM cells. Representative FACS profiles (d) and frequency (e) of LSK (lin$^-$, Sca$^+$, cKit$^+$; from left to right: $n$ = 30, 15, 21), LSK CD48$^+$ (lin$^-$, Sca$^+$, cKit$^+$, CD48$^+$; from left to right: $n$ = 28, 14, 17), LSK CD48$^-$ (lin$^-$, Sca$^+$, cKit$^+$, CD48$^-$; from left to right: $n$ = 30, 17, 20), and LSK CD48$^-$ CD34$^+$ (lin$^-$, Sca$^+$, cKit$^+$, CD48$^-$, CD34$^+$, CD135$^-$; from left to right: $n$ = 24, 14, 19), HSC$^{ST}$ (lin$^-$, Sca$^+$, cKit$^+$, CD48$^-$, CD135$^-$, CD34$^-$, CD150$^-$; from left to right: $n$ = 25, 17, 16), HSC$^{LT}$ (lin$^-$, Sca$^+$, cKit$^+$, CD48$^-$, CD135$^-$, CD34$^-$, CD150$^+$; from left to right: $n$ = 22, 17, 22) in lineage-negative fraction of BM for PBS-treated (Mock, unfilled circle) and infected mice (black square). Data obtained from distinct samples and from five independent experiments, each with at least $n$ = 3 animals per condition, are shown, and mean ± SEM is represented by a horizontal bar. Significant differences from mock are shown. ***, P < 0.001; **, P < 0.01. Absence of P value or ns, non-significant. Since data followed a normal distribution, P values were generated using Brown–Forsyth followed by ANOVA Welch test.

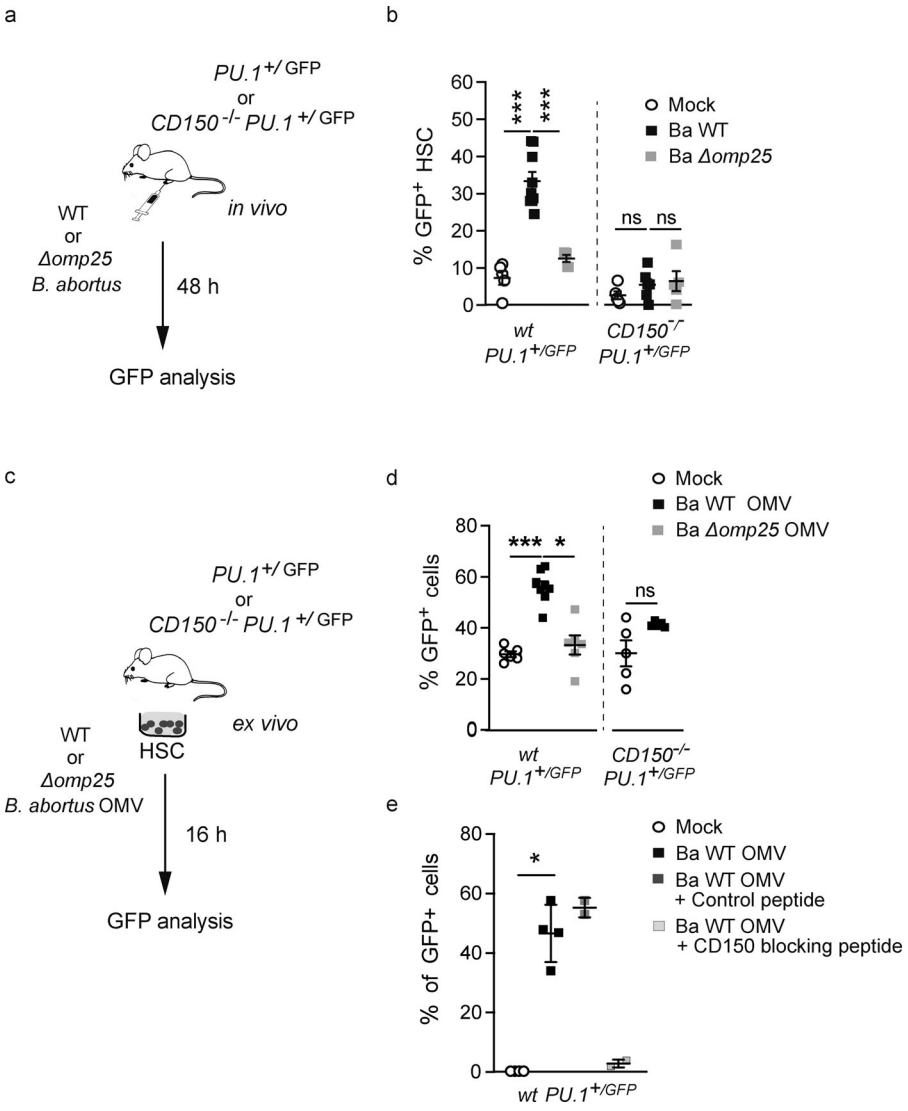


Figure 2. ***B. abortus* induces PU.1 upregulation in an Omp25/CD150-dependent manner.** **(a)** Experimental scheme: *Pu.1*$^{+/GFP}$ and *CD150*$^{-/-}$ *Pu.1*$^{+/GFP}$ mice were intraperitoneally injected with PBS (Mock, unfilled circle) or inoculated with 1 × $10^6$ CFU of Ba WT (black square), Ba Δ*omp25* (gray square). 2 d later, the percentage of GFP expression in HSC (lin$^-$, Sca$^+$, cKit$^+$, CD48$^-$, CD135$^-$ CD34$^-$) was assessed by flow cytometry. **(b)** GFP expression in BM HSC (lin$^-$, Sca$^+$, cKit$^+$, CD48$^-$, CD135$^-$, CD34$^-$) assessed by flow cytometry at day 2 after infection. Data (b) were obtained from distinct samples (from left to right, *n* = 5, 10, 5, 5, 6) from three independent experiments. Mean ± SD is represented by a horizontal bar. Significant differences from mock are shown. ***, P < 0.001; * P < 0.05. Absence of P value or ns, non-significant. Since data did not follow a normal distribution, P values were generated using Kruskal–Wallis followed by Dunn's test. **(c)** Experimental scheme: HSC (lin$^-$, Sca$^+$, cKit$^+$, CD48$^-$, CD135$^-$, CD34$^-$) from *Pu.1*$^{+/GFP}$ or *CD150*$^{-/-}$ *Pu.1*$^{+/GFP}$ mice were sorted, then stimulated ex vivo with PBS or *B. abortus* WT OMVs, *B. abortus* Δ*omp25* OMVs. After 16 h, the level of GFP in cells was assessed by flow cytometry. **(d)** Percentage of GFP + HSC 16 h after ex vivo stimulation with *B. abortus* WT OMV (black square), *B. abortus* Δ*omp25* OMV (gray square) compared to mock (Mock, unfilled circle) assessed by flow cytometry (from left to right: *n* = 6, 6, 6, 5, 5). **(e)** Percentage of GFP$^+$ HSC assessed by flow cytometry 0 h (Mock, unfilled circle, *n* = 4) or 16 h after ex vivo stimulation with *B. abortus* WT (black square, *n* = 4), *B. abortus* WT OMV and the control peptide (100 µg/ml; black square, *n* = 2), and blocking peptide of CD150 (100 µg/ml; gray square, *n* = 2). Data (d and e) were obtained from HSC of a pool of three to four mice, and the pool of cells has been divided by the number of tested conditions. Each dot is a replicative experiment. Mean ± SD is represented by a horizontal bar. Significant differences from mock are shown. **, P < 0.01; *, P < 0.05. P values were generated using Mann–Whitney test.

To further investigate whether the upregulation of PU.1 in HSC upon *B. abortus* infection is due to direct recognition of *B. abortus* Omp25 by CD150, we isolated HSC from the BM of *Pu.1*$^{+/GFP}$ mice and treated them ex vivo with outer membrane vesicles (OMV; Boigegrain et al., 2004) either from Ba WT or Ba Δ*omp25* (Fig. 2 c). 16 h after ex vivo stimulation of sorted HSC by Ba WT OMV, the number of GFP-expressing HSC increased twofold (Fig. 2 d), similar to the observations with in vivo infection of *Pu.1*$^{+/GFP}$ reporter mice (Fig. 2 b). Furthermore, upregulation of GFP-expressing HSC was abolished by either incubation of wt HSC with Ba Δ*omp25* OMV (Fig. 2 d) or of *CD150*$^{-/-}$ HSC with Ba WT OMV (Fig. 2 d), or in the presence of CD150-blocking peptide (Fig. 2 e).

Taken together, these data demonstrate that HSC can sense bacteria via direct interaction of *B. abortus* outer membrane protein Omp25 with CD150. This is the first demonstration of direct recognition of a live pathogen by HSC via CD150.

### Direct sensing of *B. abortus* by HSC induces its early commitment toward the myeloid lineage

We and others have demonstrated earlier that PU.1 upregulation in HSC is a first sign of commitment toward the myeloid lineage (Pietras et al., 2016; Mossadegh-Keller et al., 2013). PU.1 upregulation in LT-HSC is associated with a myeloid transcriptomic signature in vitro and a myeloid functional fate change in vivo (Mossadegh-Keller et al., 2013). We therefore asked if the direct interaction between HSC and *B. abortus* could induce a functional commitment of HSC toward the myeloid lineage. For this purpose, we analyzed the composition of HSC-downstream progenitors 8 d after infection in the BM. As expected, an increase in myeloid-biased MPP2/3 (lin$^-$, Sca$^+$, cKit$^+$, CD48$^+$, CD135$^-$) progenitors was observed in the BM of wt mice infected with Ba WT but not in the BM of wt mice infected with Ba Δ*omp25* or infected mice lacking CD150 (Fig. 3 a and Fig. S2 for gating strategy). By contrast, the number of lymphoid-biased

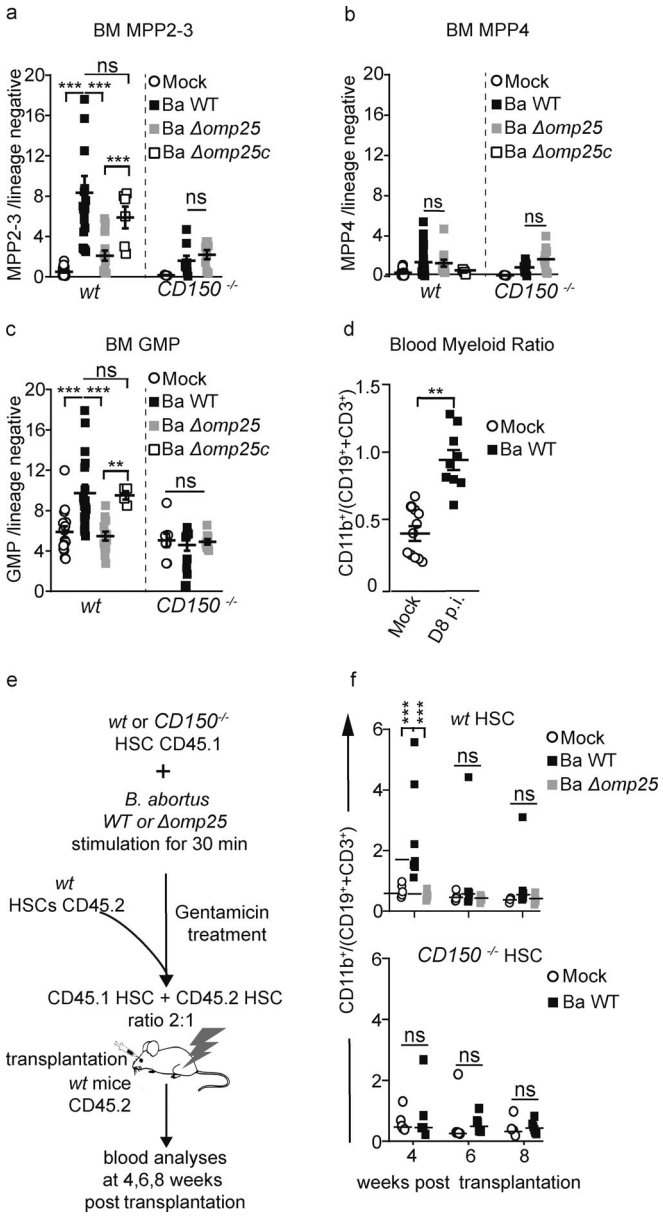


Figure 3. ***B. abortus* induces HSC differentiation towards myeloid lineage. (a–d)** C57BL/6J wt and *CD150*$^{-/-}$ mice were intraperitoneally inoculated with 1 × 10$^6$ *B. abortus* CFU. 8 d later, FACS analyses were performed for BM cells. Frequency of (a) MPP2-3 (lin$^-$, Sca$^+$, cKit$^+$ CD48$^+$, CD135$^-$; from left to right: *n* = 22, 19, 14, 6, 11, 9, 8); (b) MPP4 (lin$^-$, Sca$^+$, cKit$^+$, CD48$^+$, CD135$^+$; from left to right: *n* = 22, 21, 12, 4, 9, 9, 9); (c) GMP (lin$^-$, Sca$^-$, cKit$^+$, CD34$^+$, CD16/32$^+$; from left to right: *n* = 16, 18, 13, 4, 8, 9, 9) in lin$^-$ BM cells is shown for mice injected with PBS (Mock, unfilled circle) or inoculated with 1 × 10$^6$ CFU of Ba WT (black square), *B. abortus* Δ*omp25* (Ba Δ*omp25*; gray square), or *B. abortus* Δ*omp25* complemented with p:Omp25 (Ba Δ*omp25*c; unfilled square) mutants (the latter only for wt mice). **(d)** 8 d after infection, myeloid cells (CD45$^+$, CD11b$^+$) to lymphoid cells (CD45$^+$, CD3e$^+$; and CD45$^+$, CD19$^+$) ratio in blood is shown for mice injected with PBS (Mock; unfilled circle; *n* = 11) or inoculated with 1 × 10$^6$ CFU of Ba WT (black square; *n* = 9). **(e)** Experimental scheme: HSC from wt CD45.1 and *CD150*$^{-/-}$ CD45.1 mice were sorted and then incubated ex vivo with Ba WT or Ba Δ*omp25* for 30 min. After 30 min, cells were washed and treated for 1 h with gentamycin to kill extracellular bacteria. HSC were then transplanted into lethally irradiated wt CD45.2 recipients in competition with the CD45.2 competitor in a ratio of 2:1. FACS analyses of blood samples were performed at 4, 6, and 8 wk after transplantation. **(f)** Myeloid cells (CD45$^+$, CD11b$^+$) to lymphoid cells (CD45$^+$, CD3e$^+$; and CD45$^+$, CD19$^+$) ratio in CD45.1$^+$ blood cells is shown for hematopoietic cells provided by CD45.1$^+$ wt mice (upper panel) or *CD150*$^{-/-}$ mice (lower panel), non-infected (Mock, unfilled circle) or infected with 1 × 10$^6$ CFU of Ba WT (black circle), Ba Δ*omp25* (gray circle) as described in panel e (from left to right: for WT, *n* = 12, 13, 10, 10, 9, 9, 12, 8, 8; and for CD150$^{-/-}$, *n* = 9, 4, 14, 8, 11, 7). Data were obtained from distinct samples from four independent experiments (a–d) or from repetitive sampling from two independent experiments (e and f). Mean ± SEM is represented by a horizontal bar. Significant differences from mock are shown. ***, P < 0.001; **, P < 0.01. Absence of P value or ns, non-significant. Since data did not follow a normal distribution, P values were generated using Kruskal–Wallis followed by Dunn's test.

MPP4 (lin$^-$, Sca$^+$, cKit$^+$, CD48$^+$, CD135$^+$) was similar in infected and non-infected mice (Fig. 3 b). Moreover, analysis of downstream committed progenitors revealed an increase of GMP and blood myeloid cells (Fig. 3, c and d; and Fig. S2 for gating strategy). In addition, infection of wt mice by the Ba Δ*omp25*c complemented strain (Ba Δ*omp25* strain complemented with an Omp25-expressing plasmid) was able to rescue the increase of myeloid MPP2-3 and GMP, demonstrating a direct role of Omp25 in controlling the increase of myeloid commitment via CD150 (Fig. 3, a–c). Altogether, these data provide evidence that *B. abortus* induces an increase of myeloid cell production in an Omp25/CD150-dependent manner, though not at the expense of lymphoid cells.

HSC are known to both self-renew and differentiate to replenish the whole hematopoietic system, properties that can be tested by transplantation in an irradiated host (Weissman, 2014; Till and McCulloch, 1961). To functionally confirm that the increased production of myeloid progenitors and mature cells was initiated by direct stimulation of HSC by *B. abortus*, we co-transplanted ex vivo stimulated and unstimulated HSC in the same recipient mice. We sorted HSC (KSL, CD48$^-$, CD34$^-$, CD135$^-$) from CD45.1 *CD150*$^{-/-}$ or CD45.1 wt mice, stimulated them ex vivo with *B. abortus* for 30 min, and treated them with gentamicin to kill extracellular bacteria. We then transplanted the stimulated *CD150*$^{-/-}$ or wt HSC in competition with non-stimulated CD45.2 competitor HSC (ratio 2:1) into lethally irradiated CD45.2-recipient mice (Fig. 3 e). Blood analyses 4 wk after transplantation show that HSC stimulated with Ba WT generated more myeloid than lymphoid cells in the peripheral blood compared with non-stimulated HSC (Fig. 3 f, upper panel, and Fig. S3 for gating strategy). Again, the myeloid commitment bias of HSC was abolished when HSC were stimulated ex vivo before transplantation with Ba Δ*omp25* (Fig. 3 f, upper panel) or when *CD150*$^{-/-}$ HSC were stimulated with Ba WT (Fig. 3 f, lower panel). Furthermore, the increased myeloid to lymphoid ratio in the blood generated by Ba WT–stimulated HSC was transient and was not observed 6 and 8 wk after transplantation (Fig. 3 f, upper panel). This indicates that HSC re-equilibrate lineage commitment without compromising long-term multilineage contribution (Fig. S1 g), as is also observed for direct M-CSF stimulation of HSC (Mossadegh-Keller et al., 2013). In summary, our in vivo and ex vivo data demonstrate that HSC are able to sense directly live bacteria such as *B. abortus* via CD150 and transiently increase the production of myeloid cells in response to infection.

Inflammation induced by infection produces many signals, including cytokines, that can represent a confounding factor when establishing the effect of the direct interaction of *B. abortus* with CD150 on HSC. To address the potential indirect and confounding effect of inflammation, we generated mixed hematopoietic chimera mice by transplanting a 1:1 mix of BM cells from wt CD45.2 mice and *CD150*$^{-/-}$ CD45.1 mice into irradiated CD45.2-recipient mice (Fig. 4 a). This allowed investigation of both wt HSC and *CD150*$^{-/-}$ HSC in the same inflammatory environment. 12 wk after transplantation, we infected chimeric mice with *B. abortus*. The overall chimerism was still 1:1 12 wk after transplantation and 12 wk plus 1 wk after infection (Fig. 4 b). We then assessed the HSC lineage output in CD45.2 (wt) and CD45.1 (*CD150*$^{-/-}$) compartments by analyzing, from the same recipients, the myeloid/lymphoid ratio in mature blood cells and BM progenitors (Fig. 4, c–f). 8 d after infection with Ba WT, the blood myeloid/lymphoid ratio was higher in the wt compartment compared with the *CD150*$^{-/-}$ compartment from the same recipient mice (Fig. 4 c, middle panel). Although both Ba WT and Ba Δ*omp25* have equal virulence (Fig. S1 f), the increase of blood myeloid/lymphoid ratio in the wt compartment was abolished upon Ba Δ*omp25* infection of chimeric mice (Fig. 4 c, right panel). Furthermore, myeloid-biased MPP2-3 cells (Fig. 4 e) as well as GMP (Fig. 4 d) were also increased in an Omp25/CD150-dependent manner. By contrast, Omp25/CD150 interaction did not perturb the number of lymphoid-biased multipotent progenitors MPP4 (Fig. 4 f).

Together, these results confirm that myeloid commitment induced by *B. abortus* was intrinsic to HSC and due to direct Omp25/CD150 interaction and not to indirect effects of confounding additional inflammatory signals.

### Physio-pathological consequences of chronic stimulation of HSC by *B. abortus*

To address the long-term consequences of CD150-Omp25 mediated sensing of *B. abortus* by HSC, we first analyzed the number of HSC in mice 30 d after infection with Ba WT or Ba Δ*Omp25*, when the infection is chronically installed in the BM (Fig. 4, g–i). In contrast to acute infection (at day 2 and 8; Fig. 1 e), chronic infection (at day 30 after infection) triggered HSC loss in the BM (Fig. 4 i), the loss being slightly less pronounced in wt mice infected with Ba Δ*Omp25* or in *CD150*$^{-/-}$ mice. These results attest that chronic stimulation of HSC by *B. abortus* does affect HSC function. To further address the long-term repopulating potential of HSC upon chronic infection, we performed competitive transplantation experiments using HSC from chronically infected mice. For this, we transplanted irradiated CD45.2 hosts with a 1:1 ratio of lin$^-$ BM cells from CD45.1 mice 30 d after infection with Ba WT or Ba Δ*Omp25* and lin$^-$ BM competitor cells from non-infected wt CD45.2 mice (Fig. 4 j). Peripheral blood analysis of donor-derived hematopoietic cells, up to 8 wk after transplantation, revealed that HSC from mice chronically infected with Ba WT have partially lost their reconstitution potential compared with HSC from non-infected mice or mice infected with Ba Δ*Omp25* (Fig. 4 k). Together, these results indicate that chronic infection with *B. abortus* affects the long-term functions of HSC.

In humans, infection with several pathogens is sometimes associated with reduced red blood cell generation leading to the acute arrest of hematopoiesis (Bi et al., 2016). Interestingly, in *B. abortus*–infected wt mice the percentage of erythroid progenitors (MEP) in the BM decreases in an Omp25/CD150-dependent manner (Fig. 5 a). To investigate if the reduced level of MEP results in anemia, wt and *CD150*$^{-/-}$ mice were infected with *B. abortus* and 8 d after infection, the hematocrit was measured (Fig. 5 b). Furthermore, the hematocrit of infected mice was reduced compared with non-infected mice but was rescued in mice infected with *Ba ΔOmp25* and in *CD150*$^{-/-}$ mice (Fig. 5 b).

These results indicate that in addition to an increased myeloid commitment, reduced production of red cells at the level of progenitors is a consequence of Omp25/CD150-dependent interaction during the infection process. Consistent with these observations, a significant proportion of human brucellosis patients also shows anemia (Fig. 5 c). It is therefore not surprising that anemia can be observed in both infected mice and in human brucellosis patients.

### Is CD150-Omp25–mediated sensing of *B. abortus* by HSC protective or detrimental to the organism?

This study raises the question of how the recognition of CD150 by pathogens that induce myelopoiesis may benefit or harm either the host or the pathogen.

We have demonstrated earlier that short-term stimulation with either LPS or M-CSF induces myeloid commitment of HSC and transient myeloid cell production without affecting the long-term repopulation function of HSC (Mossadegh-Keller et al., 2013; de Laval et al., 2020). This transient boost of myeloid cell production from stimulated HSC could be exploited to protect immune-compromised patients from infections with opportunistic pathogens (Kandalla et al., 2016). Here, we have demonstrated that direct sensing of *B. abortus* by HSC via the CD150-Omp25 interaction also leads to increased myelopoiesis in the acute phase of the disease (day 8) or after a short ex vivo stimulation (30 min) without inducing any loss of HSC function. It is thus possible that short-term sensing of bacteria by HSC via CD150, even through other Omps than Omp25 of *B. abortus*, or of viruses (since CD150 is a receptor for measles virus) could be beneficial to the host, as LPS or M-CSF stimulation is. On the other hand, for some pathogens, HSPC expansion is detrimental to the host and beneficial to the pathogen (Abidin et al., 2017). We have observed that during the chronic phase of the disease, the persistence of *B. abortus* in vivo lasting over 30 d induces a chronic stimulation of HSC by *B. abortus* that leads to a loss of HSC function (Fig. 4 k), demonstrating that long-term *B. abortus* infection is rather detrimental for the host. The consequences of pathogen sensing via CD150 on HSC functions will therefore likely depend on the nature of the pathogen and the duration of the interaction to result in either protective or detrimental effects. Moreover, the molecular mechanisms downstream of CD150 in HSC upon *B. abortus* sensing remain to be elucidated.

Enhanced myeloid production has been shown to promote pathogen clearance of *Escherichia coli* and *Salmonella* Typhimurium (Takizawa et al., 2012). Moreover, *CD150*$^{-/-}$ mice are protected from *Trypanosoma cruzi* lethal challenge but are sensitive to *Leishmania major* and attenuated *Salmonella* Typhimurium (Silverberg et al., 2001), suggesting a beneficial role for CD150 in

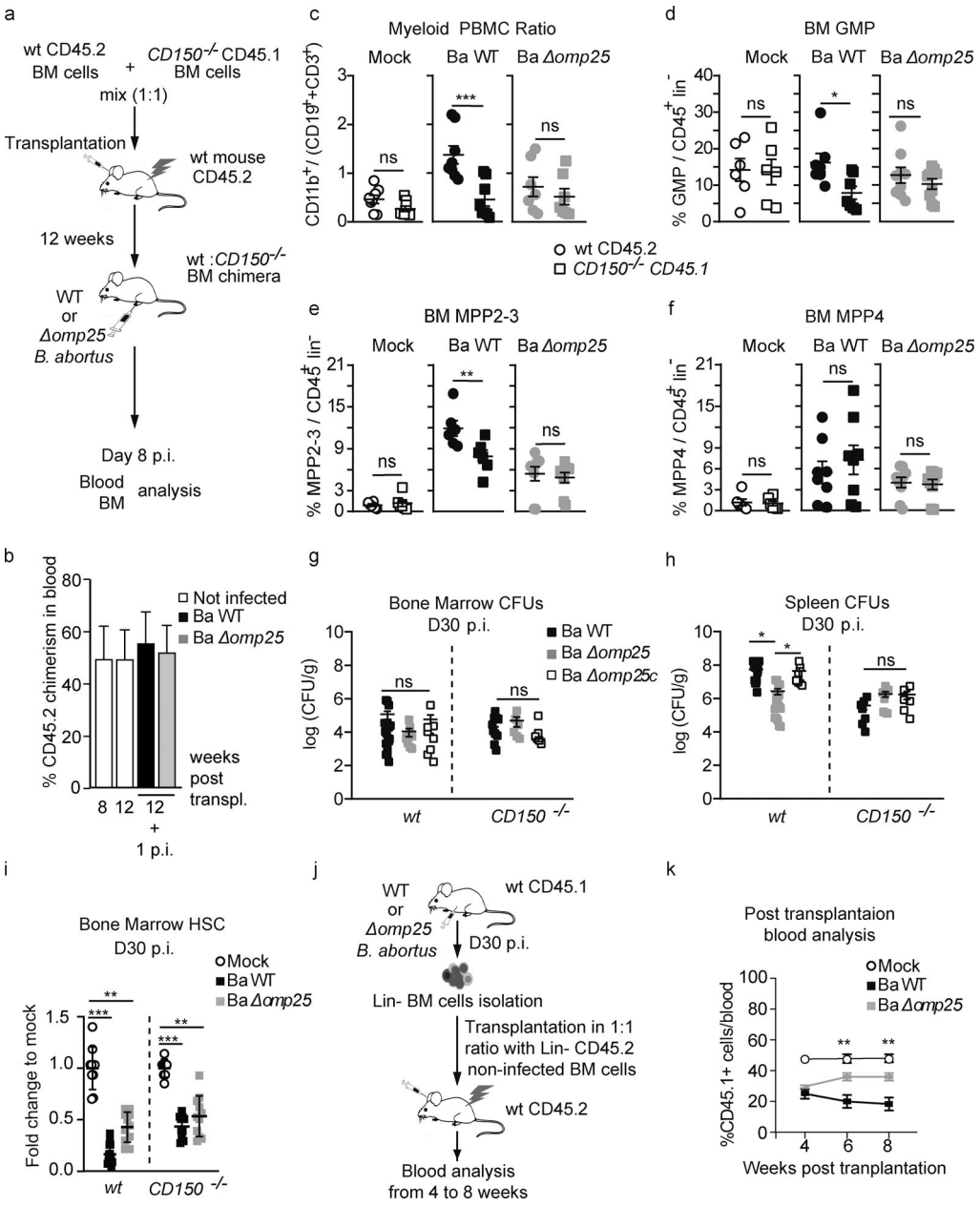


Figure 4. **HSC myeloid bias induced by *B. abortus* Omp25/CD150 interaction is hematopoietic cell autonomous. (a)** Experimental scheme: BM cells from *CD150*$^{-/-}$ CD45.1 mice and wt CD45.2 mice were isolated from mouse tibiae and femurs and transplanted in a 1:1 ratio into lethally irradiated recipient CD45.2 mice. 12 wk after transplantation, wt CD45.2:*CD150*$^{-/-}$ CD45.1 chimeric mice were intraperitoneally injected with PBS (Mock, unfilled circle) or inoculated with 1 × $10^6$ CFU of Ba WT, *B. abortus* Δ*omp25* (Ba Δ*omp25*). Blood and BM were analyzed 8 d later. **(b)** Overall blood chimerism was obtained 8 and 12 wk after reconstitution and 1 wk after infection with Ba WT (black square) and Ba Δ*omp25* (gray square). **(c–f)** Myeloid (CD45$^+$, CD11b$^+$ cells) to lymphoid (CD45$^+$, CD3e$^+$; and CD45$^+$, CD19$^+$) ratio in the blood (from left to right: *n* = 8, 8, 8, 8, 7, 7); frequency of (d) GMP (from left to right: *n* = 6, 6, 7, 7, 9, 9), (e) MPP2-3 (from left to right: *n* = 6, 6, 6, 6, 9, 9), and (f) MPP4 (from left to right: *n* = 6, 6, 8, 8, 9, 9) in BM lin$^-$ cells of wt CD45.2 (circle) and *CD150*$^{-/-}$ CD45.1 (square) compartment is shown for chimeric mice intraperitoneal injected with PBS (Mock, unfilled symbols) or inoculated with 1 × $10^6$ CFU of Ba WT (symbol filled in black) or Ba Δ*omp25* (symbol filled in gray). **(g and h)** CFU count per gram of organ at day 30 after infection of wt CD45.1 and *CD150*$^{-/-}$ CD45.1 mice for (g) BM (from left to right: *n* = 18, 9, 8, 12, 6, 6) and (h) spleen (from left to right: *n* = 14, 18, 7, 7, 8, 6) infected with Ba WT (black square), Ba Δ*omp25* (gray square), or *B. abortus* Δ*omp25* complemented with p:Omp25 (Ba Δ*omp25c*; unfilled square). **(i)** Fold change of HSC absolute number in mice at day 30 after infection (D30 p.i.) with indicated bacteria (from left to right: *n* = 9, 14, 11, 8, 11, 11). Data were obtained from distinct samples from three independent experiments. **(j)** Experimental scheme: wt CD45.1 mice were intraperitoneally inoculated with 1 × $10^6$ CFU of Ba WT. BM cells were isolated from femurs and tibiae of the infected mice at day 30 after infection, and lin$^-$ cells were sorted and analyzed by FACS and transplanted in a 1:1 ratio with lin$^-$ cells from wt CD45.2 non-infected mice into previously lethally irradiated wt CD45.2-recipient mice. FACS analyses on blood were performed at 4, 6, and 8 wk after transplantation. **(k)** Contribution of CD45.1 cells from infected mice to blood chimerism in CD45.2 recipients at 4, 6, and 8 wk after transplantation (mock, *n* = 5; Ba WT, *n* = 7; Ba Δ*omp25*, *n* = 7). Data were obtained from two independent experiments. Mean ± SEM is represented by a horizontal bar. Significant differences from mock are shown. ***, P < 0.001; **, P < 0.01; *, P < 0.05. Absence of P value or ns, non-significant. Since data did not follow a normal distribution, P values were generated using Kruskal–Wallis followed by Dunn's test.

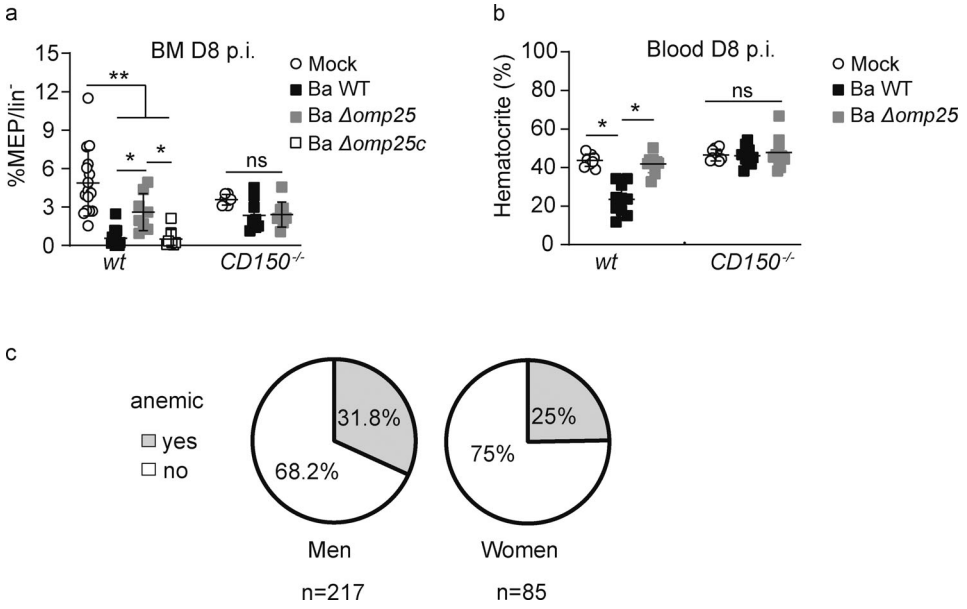


Figure 5. ***B. abortus* infection induces anemia in both human and mice. (a and b)** wt CD45.1 and *CD150*$^{-/-}$ CD45.1 mice were intraperitoneally inoculated with 1 × $10^6$ CFU of *B. abortus*. **(a)** Frequency of MEP (lin$^-$, Sca$^-$, cKit$^+$, CD34$^-$, CD16/32$^-$), in lin$^-$ BM cells 8 d after infection is shown for mice injected with PBS (Mock, unfilled circle) or inoculated with 1 × $10^6$ CFU of Ba WT (black square), *B. abortus* Δ*omp25* (Ba Δ*omp25*; gray square), or *B. abortus* Δ*omp25* complemented with p:Omp25 (Ba Δ*omp25*c; unfilled square) mutants (the latter only for wt mice; from left to right: *n* = 16, 16, 8, 8, 8, 7, 9). **(b)** 8 d after infection, the percentage of hematocrit measured in blood is shown for mice injected with PBS (Mock, unfilled circle) or inoculated with 1 × $10^6$ CFU of Ba WT (black square), Ba Δ*omp25* (gray square; from left to right:, *n* = 7, 7, 6, 5, 8, 8). Data were obtained from distinct samples from three independent experiments (a and b), each with at least *n* = 4 animals per condition, are shown and mean ± SEM is represented by a horizontal bar. Significant differences from mock are shown. **, P < 0.01; *, P < 0.05. Absence of P value or ns, non-significant. Since data did not follow a normal distribution, P values were generated using Kruskal–Wallis followed by Dunn's test. **(c)** Percentage of brucellosis patients (men and women) that present anemia before antibiotic treatment. Anemia was characterized by a decrease of hematocrit, hemoglobin, and erythrocytes (hematocrit <40% for men and <35% for women; hemoglobin <14 g/dl for men and <12 g/dl for women; erythrocyte count <4 million for men and <3.8 million/mm$^3$ for women).

response to some infections. However, in this study, we have shown that during the chronic phase of the disease (day 30) in the spleen, the natural reservoir in mice for *B. abortus*, the bacterial load was decreased in *CD150*$^{-/-}$ mice and in wt mice infected with Ba Δ*Omp25* (Fig. 4 h). This suggests that the enhanced transient myeloid commitment induced by Omp25/CD150 at day 8 is more likely to be beneficial to the bacterium. Indeed, since *B. abortus* infects and replicates in myeloid cells (Salcedo et al., 2013, Gutiérrez-Jiménez et al., 2018), *B. abortus*–induced myelopoiesis in HSC increases the number of potential target cells and constitutes a bacterial advantage for dissemination and chronic infection. The Omp25/CD150 axis can thus be considered a new evasion strategy exploited by *B. abortus* to mediate its dissemination.

In conclusion, we present a novel finding demonstrating that CD150 is a bacterial sensor for HSC. How chronic activation of HSC by *B. abortus* could affect the long-term function of HSC and the role of CD150 in HSC of patients experiencing a microbial challenge would be worth investigating in the future.

## Materials and methods

### Ethics

Animal experimentation was conducted in strict compliance with good animal practice as defined by the French Animal Welfare Bodies (Law 87–848 dated October 19, 1987, modified by Decree 2001-464 and Decree 2001-131 relative to European Convention, EEC Directive 86/609). Institut National de la Santé et de la Recherche Médicale guidelines have been followed regarding animal experimentation (authorization no. 02875 for mouse experimentation). All animal work was approved by the Direction Départementale des Services Vétérinaires des Bouches du Rhône and the Regional Ethic Committee (authorization number 13.118). Authorization of *B. abortus* experimentation in the Biosafety Level 3 (BSL3) facility was given under the numbers AMO-076712016-5, AMO-076712016-6, and AMO-076712016-7. All efforts were made to minimize suffering during animal handling and experimentation.

The human study was approved by the Ethics Committee of the Medical Faculty in Skopje, Republic of North Macedonia (no. 03-7670/2). The laboratory data presented were obtained as part of a routine diagnostic protocol, and written informed consent was obtained from all patients. The values of red blood cells, hematocrit, and hemoglobin were retrospectively analyzed in 302 patients with human brucellosis before therapy was initiated. The patients were managed at the University Clinic of Infectious Diseases and Febrile Conditions in Skopje from 2007 to 2018. 217 men and 85 women with a median age of 39 (range 3–79) years were studied. The diagnosis of brucellosis was based on the clinical signs and symptoms compatible with brucellosis (arthralgia, fever, sweating, malaise, hepatomegaly, splenomegaly, and signs of focal disease) confirmed by a qualitative

positive Rose Bengal test and a Brucellacapt assay of >1/320. Hemoglobin thresholds used to define anemia were according to the World Health Organization (World Health Organization, 2008).

### Mice

6–10 wk-old C57BL/6J females (Charles River), *CD150*$^{-/-}$ mice (kindly provided by Yusuke Yanagi, Department of Virology, Faculty of Medicine, Kyushu University, Fukuoka, Japan; Davidson et al., 2004) or Pu.1$^{+/GFP}$ mice (Back et al., 2004; Bryder et al., 2006), both on a C57BL/6J background, were used. Animals were housed in cages with water and food ad libitum in the Centre d'Immunophénomique (CIPHE) animal house facility, Marseille. 2 wk before the start of experiments, mice were transferred to the BSL3, CIPHE, Marseille, and kept under strict biosafety containment conditions all along with infection with live bacteria.

### Bacterial strains

*B. abortus* 2308 (Ba WT), *B. abortus Δomp25* (kanR; Ba *Δomp25*), or *B. abortus Δomp25c:pOmp25* (kanR, AmpR; Ba *Δomp25c*) were used for infection. Ba *Δomp25* was a gift from Pr. Ignacio Moriyón, University of Navarra, Pamplona, Spain.

### *B. abortus* infection

Mice were inoculated intraperitoneally with 1 × $10^6$ CFU in 100 µl of PBS for each *B. abortus* strain. Strains were grown in tryptic soy agar (Sigma-Aldrich) for 5 d, then overnight at 37°C for 16 h under shaking in tryptic soy broth (Sigma-Aldrich) with 25 µg/ml kanamycin for Ba *Δomp25* until the OD (OD at 600 nm) reached 1.8 or kanamycin and ampicillin at 50 µg/ml for the Ba *Δomp25pBBR4omp25* strain. All *B. abortus* were kept, grown, and used under strict biosafety containment conditions all along experiments in the BSL3 facility, CIPHE, Marseille. For CFU, enumeration at different time points after infection, spleen and BM were collected (Gutiérrez-Jiménez et al., 2018). Femurs and tibiae were flushed with 500 µl of ice-cold PBS to isolate BM cells. BM cell suspension was then plated in tryptic soy agar plates. Spleens were collected and splenocytes were isolated by mechanical disruption.

Organs were harvested at 2, 8, or 30 d after infection, weighted, and then dissociated into sterile endotoxin-free PBS. Serial dilutions in sterile PBS were used to count CFU. Serial dilutions were plated in triplicates onto tryptic soy broth agar to enumerate CFU after 3 d at 37°C.

### Transplantation assays

All donor cells were from *CD150*$^{+/+}$ and *CD150*$^{-/-}$ CD45.1 mice and transplanted into lethally irradiated (5.9 Gy) CD45.2-recipient mice. For competitive assays, mice were transplanted with equal numbers of 1 × $10^6$ total BM cells or 1 × $10^6$ lineage negative cells. For infected HSC transplantation, 1,000 sorted HSC (KSL, CD48$^-$, CD135$^-$, CD34$^-$) were infected with Ba WT or Ba *Δomp25* at a multiplicity of infection of 30:1. Bacteria were centrifuged onto cells at 400 *g* for 10 min at 15°C and then incubated for 30 min at 37°C under 5% $CO_2$. Cells were washed twice with medium and then incubated for 1 h in medium containing 100 µg/ml gentamicin (Sigma-Aldrich) to kill extracellular bacteria (absence of persistent live bacteria was assessed by CFU assays). Cells were then washed three times with PBS. Infected cells were mixed in a 1:1 ratio with non-infected HSC before transplantation. Hematopoietic reconstitution and lineage determination were monitored at 4, 6, and 8 wk after transplantation in the peripheral blood. 8 wk after transplantation, mice were sacrificed, and tibiae and femurs were harvested. BM cells were flushed from the femur and tibiae and resuspended in FACS media (PBS, 2% FCS, 5 mM EDTA) for flow cytometry analyses.

### Flow cytometry

For FACS sorting and analysis, we used a FACSAriaIII or a LSR-X20 (BD) and the FlowJo software v10 (Treestar). For HSC and progenitor analysis, total BM cells were depleted of mature cells using a direct lineage depletion kit (Miltenyi Biotec) and stained with antibodies anti-CD34-APC or anti-BV421 (cloneRAM34; BD Bioscience), anti-CD135-PE-CF594 or anti-PE (clone A2F10.1; BD Bioscience), anti-CD150-PE-Cy7 or anti-BV711 (clone TC15-12F12.2; BioLegend), anti-CD117-BV605 (clone 2B8; BioLegend), anti-Sca-1-PrcpCy5.5 or anti-PE (clone D7; Thermo Fisher Scientific), anti-CD48-BV510 or anti-PE-Cy7 (clone HM48-1; BD Bioscience), and anti-CD16/32-PE or anti-APC-Cy7 (clone 2.4G2; BD Bioscience). To improve the analysis and enumeration of HSC/MPP populations by FACS in infected mice, we used CD48 as an extra marker to eliminate LSK,c-Kit$^+$ progenitors that could pollute HSC/MPP gates because of some re-expressing Sca-1 upon stimulation by infection. When needed, anti-CD45.1-APC or anti-BV421 (clone A20; BD Bioscience) and anti-CD45.2-FITC or anti-PrcpCy5.5 (clone 104; BD Bioscience) were added. LIVE/DEAD (UV Fixable Blue Dead Cell Stain, Thermo Fisher Scientific) was used as a viability marker. For biosafety reasons, stained infected cells were finally fixed for 20 min with Antigen Fix at room temperature prior to acquisition.

Blood cells were stained with anti-CD11b FITC (clone M1/70; eBioscience), anti-CD19-PE-Cy7 (clone 6D5; BioLegend), anti-CD45.2-PrcpCy5.5 (clone 104; BD Bioscience), anti-CD45.1-BV421 (clone A20; BD Bioscience), anti-CD3e-APC (clone 145-2C11; BD Bioscience), and anti-Ly6G-PE (clone 1A8; BD Bioscience). Red blood cells were lysed using BD FACS lysing solution (BD) for 20 min then fixed for 10 min with Antigen Fix at room temperature prior to acquisition.

### HSC ex vivo challenge with *B. abortus* outer membrane extracts

All cultures were performed at 37°C under 5% $CO_2$. Sorted HSC from wt or *CD150*$^{-/-}$ mice were cultured in StemSpan SFEMII (Stem Cells) complemented with 50 ng/µl TPO (Peprotech) and 20 ng/µl SCF (Peprotech). Cells were stimulated with *B. abortus* outer membrane extracts from Ba WT or with Ba *Δomp25* (10 µg/ml). *B. abortus* outer membrane extracts were a gift from Pr. Ignacio Moriyón, University of Navarra, Pamplona, Spain.

Sorted HSC were also cultured with blocking CD150 peptide (FCKQLKLYEQVSPPE, 100 µg/ml; Auspep) or control peptide (DLSKGSYPDHLEDGY, Auspep, 100 µg/ml; Thermo Fisher Scientific).

### HSC and progenitor cells ex vivo infection with *B. abortus*

HSC ($lin^-$, $Sca^+$, $cKit^+$, $CD48^-$, $CD135^-$, $CD34^-$), MPP ($lin^-$, $Sca^+$, $cKit^+$, $CD48^+$), GMP ($lin^-$, $Sca^+$, $cKit^+$, C16/$32^+$, $CD34^-$), and MEP ($lin^-$, $Sca^+$, $cKit^+$, C16/$32^-$, $CD34^+$) were sorted using FACS Aria. Cells were resuspended in StemSpan SFEMII (Stem Cells) complemented with 50 ng/µl TPO (Peprotech) and 20 ng/µl SCF (Peprotech) and transferred into the BSL3 to be infected with Ba WT or Ba *Δomp25* at a multiplicity of infection of 30:1. Bacteria were centrifuged onto cells at 400 *g* for 10 min at 15°C and then incubated for 120 min at 37°C under 5% $CO_2$, washed twice with medium, and then incubated for 1 h in medium containing 100 µg/ml gentamicin (Sigma-Aldrich) to kill extracellular bacteria. Cells were then washed three times with PBS. Infected cells were cultured in StemSpan SFEMII (Stem Cells) complemented with 50 µg/ml gentamicin (Sigma-Aldrich), 50 ng/µl TPO (Peprotech), and 20 ng/µl SCF (Peprotech). 24 h after infection, cells were washed three times with PBS and processed for bacterial CFU or confocal imaging. Cells were plated in tryptic soy agar plates for CFU enumeration at different time points after infection. For confocal microscopy, cells were fixed with AntigenFix for 30 min at room temperature, washed with PBS-Triton 0.01%, and mounted on coverslips using ProlongGold AntiFade Mountant with DAPI (P36931; Thermo Fisher Scientific).

### Statistics

Results were evaluated by GraphPad Prism 8 software (GraphPad Software). Statistical tests used are indicated in the figure legends. A value of *, $P < 0.05$ was determined as significant.

### Software

GraphPad Prism 9 was used for data visualization. Fiji/ImageJ (V) software 2.1.0/1.53c was used for confocal microscopy analysis. FlowJo software 10.7.1 was used for flow cytometry analysis.

### Online supplemental material

Fig. S1 shows the number of CFU in the BM and spleen of mice infected with *B. abortus* or transplanted with BM from infected mice and the number of BM and $lin^-$ cells in wt and *CD150*$^{-/-}$ animals after infection with Mock, Ba WT, Ba *Δomp25*, and Ba Δomp25c. Fig. S2 shows the FACS gating strategy used to analyze HSC and progenitor cells in BM. Fig. S3 shows the FACS gating strategy used to analyze mature cells in the blood of transplanted mice.

### Data availability

No datasets were generated during the current study.

## Acknowledgments

We thank all the staff of the Centre d'Immunologie de Marseille-Luminy (CIML) and CIPHE mouse facilities, Marc Barad, Sylvain Bigot of the CIML flow cytometry facility, Dr. Hervé Luche, Pierre Grenot of the CIPHE flow cytometry facility, and Claude Napez and Philippe Hoest of the CIPHE BSL3 facility. We acknowledge Pr. Ignacio Moriyón (University of Navarra, Pamplona, Spain) for the generous gift of mutant *B. abortus* strains as well as *B. abortus* outer membrane preparations, and Dr. Yusuke Yanagi and Dr. Masato Kubo for providing us with *CD150*$^{-/-}$ CD45.1 mice. We thank Dr. Taymour Hamoudi from the University of California, San Francisco, for critical reading of the manuscript and Dr. Sylvie Memet and Dr. Guillaume Hoeffel for discussions about this work.

This study was supported by institutional grants from the Institut National de la Santé et de la Recherche Médicale, Centre National de la Recherche Scientifique, and Aix-Marseille University to CIML; grants to J.P. Gorvel from the Fondation pour la Recherche Médicale (FRM grant number DQ20170336745), the Agence Nationale de Recherche/Investissements d'Avenir–Labex INFORM (ANR-11-LABX-0054), and Agence Nationale de Recherche/Investissements d'Avenir–A*MIDEX (ANR-11-IDEX-0001-02); grants to S. Sarrazin from ITMO Cancer Aviesan (Alliance Nationale pour les Sciences de la Vie et de la Santé, National Alliance for Life Science and Health) within the framework of the Cancer Plan (ISC19032ASA); and grants to M.H. Sieweke from the Agence Nationale pour la Recherche (ANR-17-CE15-0007-01 and ANR-18-CE12-0019-03), Fondation ARC pour la Recherche sur le Cancer (PGA1 RF20170205515), an INSERM-Helmholtz cooperation and the European Research Council under the European Union's Horizon 2020 research and innovation program (grant agreement number 695093 MacAge). L. Hysenaj received a fellowship from Investissements d'Avenir–Labex INFORM, and B. de Laval received a fellowship from the Fondation ARC. M.H. Sieweke was supported as a Berlin Institute of Health Einstein visiting fellow at the Max Delbrück Center and is an Alexander von Humboldt Professor at TU Dresden.

Author contributions: J.P. Gorvel, M.H. Sieweke, and S. Sarrazin conceived, and J.P. Gorvel and S. Sarrazin supervised the study. J.P. Gorvel, M.H. Sieweke, and S. Sarrazin got the financial support for the project. J.P. Gorvel, M.H. Sieweke, S. Sarrazin, L. Hysenaj, B. de Laval, and V. Arce-Gorvel designed the experiments. L. Hysenaj, G. González-Espinoza, and V. Arce-Gorvel performed all BSL3 experiments and L. Hysenaj, B. de Laval, and G. Debroas performed experiments not requiring a BSL3 facility. M. Bosilkovski was responsible for human studies. J.P. Gorvel, M.H. Sieweke, S. Sarrazin, L. Hysenaj, B. de Laval, and V. Arce-Gorvel interpreted the data. S. Sarrazin, L. Hysenaj, B. de Laval, J.P. Gorvel, M.H. Sieweke, and V. Arce-Gorvel wrote the original manuscript. S. Sarrazin, B. de Laval, J.P. Gorvel, M.H. Sieweke, and V. Arce-Gorvel reviewed the original manuscript. S. Sarrazin and B. de Laval edited the final manuscript.

Disclosures: The authors declare no competing interests exist.

Submitted: 9 March 2021
Revised: 5 January 2023
Accepted: 13 March 2023

## References

Abidin, B.M., A. Hammami, S. Stäger, and K.M. Heinonen. 2017. Infection-adapted emergency hematopoiesis promotes visceral leishmaniasis. *PLoS Pathog.* 13:e1006422. https://doi.org/10.1371/journal.ppat.1006422

Allen, M.B., B.S. Pritt, L.M. Sloan, C.D. Paddock, C.K. Musham, J.M. Ramos, N. Cetin, and E.R. Rosenbaum. 2014. First reported case of Ehrlichia

ewingii involving human bone marrow. *J. Clin. Microbiol.* 52:4102–4104. https://doi.org/10.1128/JCM.01670-14

Back, J., A. Dierich, C. Bronn, P. Kastner, and S. Chan. 2004. PU.1 determines the self-renewal capacity of erythroid progenitor cells. *Blood*. 103: 3615–3623. https://doi.org/10.1182/blood-2003-11-4089

Berger, S.B., X. Romero, C. Ma, G. Wang, W.A. Faubion, G. Liao, E. Compeer, M. Keszei, L. Rameh, N. Wang, et al. 2010. SLAM is a microbial sensor that regulates bacterial phagosome functions in macrophages. *Nat. Immunol.* 11:920–927. https://doi.org/10.1038/ni.1931

Bi, L., J. Li, Z. Lu, H. Shao, and Y. Wang. 2016. Acute arrest of hematopoiesis induced by infection with Staphylococcus epidermidis following total knee arthroplasty: A case report and literature review. *Exp. Ther. Med.* 11:957–960. https://doi.org/10.3892/etm.2016.3023

Boettcher, S., R.C. Gerosa, R. Radpour, J. Bauer, F. Ampenberger, M. Heikenwalder, M. Kopf, and M.G. Manz. 2014. Endothelial cells translate pathogen signals into G-CSF-driven emergency granulopoiesis. *Blood*. 124:1393–1403. https://doi.org/10.1182/blood-2014-04-570762

Boettcher, S., and M.G. Manz. 2017. Regulation of inflammation- and infection-driven hematopoiesis. *Trends Immunol.* 38:345–357. https://doi.org/10.1016/j.it.2017.01.004

Boigegrain, R.A., I. Salhi, M.T. Alvarez-Martinez, J. Machold, Y. Fedon, M. Arpagaus, C. Weise, M. Rittig, and B. Rouot. 2004. Release of periplasmic proteins of Brucella suis upon acidic shock involves the outer membrane protein Omp25. *Infect. Immun.* 72:5693–5703. https://doi.org/10.1128/IAI.72.10.5693-5703.2004

Bryder, D., D.J. Rossi, and I.L. Weissman. 2006. Hematopoietic stem cells: The paradigmatic tissue-specific stem cell. *Am. J. Pathol.* 169:338–346. https://doi.org/10.2353/ajpath.2006.060312

Burberry, A., M.Y. Zeng, L. Ding, I. Wicks, N. Inohara, S.J. Morrison, and G. Núñez. 2014. Infection mobilizes hematopoietic stem cells through cooperative NOD-like receptor and Toll-like receptor signaling. *Cell Host Microbe*. 15:779–791. https://doi.org/10.1016/j.chom.2014.05.004

Davidson, D., X. Shi, S. Zhang, H. Wang, M. Nemer, N. Ono, S. Ohno, Y. Yanagi, and A. Veillette. 2004. Genetic evidence linking SAP, the X-linked lymphoproliferative gene product, to Src-related kinase FynT in T(H)2 cytokine regulation. *Immunity*. 21:707–717. https://doi.org/10.1016/j.immuni.2004.10.005

de Laval, B., J. Maurizio, P.K. Kandalla, G. Brisou, L. Simonnet, C. Huber, G. Gimenez, O. Matcovitch-Natan, S. Reinhardt, E. David, et al. 2020. C/EBPβ-Dependent Epigenetic memory induces trained immunity in hematopoietic stem cells. *Cell Stem Cell*. 26:657–674.e8. https://doi.org/10.1016/j.stem.2020.01.017

Degos, C., L. Hysenaj, G. Gonzalez-Espinoza, V. Arce-Gorvel, A. Gagnaire, A. Papadopoulos, K.A. Pasquevich, S. Méresse, J. Cassataro, S. Mémet, and J.P. Gorvel. 2020. Omp25-dependent engagement of SLAMF1 by Brucella abortus in dendritic cells limits acute inflammation and favours bacterial persistence in vivo. *Cell. Microbiol.* 22:e13164. https://doi.org/10.1111/cmi.13164

Eldin, C., C. Melenotte, M. Million, S. Cammilleri, A. Sotto, A. Elsendoorn, F. Thuny, H. Lepidi, F. Roblot, T. Weitten, et al. 2016. 18F-FDG PET/CT as a central tool in the shift from chronic Q fever to coxiella burnetii persistent focalized infection: A consecutive case series. *Medicine*. 95:e4287. https://doi.org/10.1097/MD.0000000000004287

Erlenhoefer, C., W.J. Wurzer, S. Löffler, S. Schneider-Schaulies, V. ter Meulen, and J. Schneider-Schaulies. 2001. CD150 (SLAM) is a receptor for measles virus but is not involved in viral contact-mediated proliferation inhibition. *J. Virol.* 75:4499–4505. https://doi.org/10.1128/JVI.75.10.4499-4505.2001

Franco, M.P., M. Mulder, R.H. Gilman, and H.L. Smits. 2007. Human brucellosis. *Lancet Infect. Dis.* 7:775–786. https://doi.org/10.1016/S1473-3099(07)70286-4

Gutiérrez-Jiménez, C., L. Hysenaj, A. Alfaro-Alarcón, R. Mora-Cartín, V. Arce-Gorvel, E. Moreno, J.P. Gorvel, and E. Barquero-Calvo. 2018. Persistence of Brucella abortus in the bone marrow of infected mice. *J. Immunol. Res.* 2018:5370414. https://doi.org/10.1155/2018/5370414

Hardy, J., P. Chu, and C.H. Contag. 2009. Foci of Listeria monocytogenes persist in the bone marrow. *Dis. Model. Mech.* 2:39–46. https://doi.org/10.1242/dmm.000836

Kandalla, P.K., S. Sarrazin, K. Molawi, C. Berruyer, D. Redelberger, A. Favel, C. Bordi, S. de Bentzmann, and M.H. Sieweke. 2016. M-CSF improves protection against bacterial and fungal infections after hematopoietic stem/progenitor cell transplantation. *J. Exp. Med.* 213:2269–2279. https://doi.org/10.1084/jem.20151975

Kiel, M.J., Ö.H. Yilmaz, T. Iwashita, O.H. Yilmaz, C. Terhorst, and S.J. Morrison. 2005. SLAM family receptors distinguish hematopoietic stem and progenitor cells and reveal endothelial niches for stem cells. *Cell*. 121: 1109–1121. https://doi.org/10.1016/j.cell.2005.05.026

Kobayashi, H., C.I. Kobayashi, A. Nakamura-Ishizu, D. Karigane, H. Haeno, K.N. Yamamoto, T. Sato, T. Ohteki, Y. Hayakawa, G.N. Barber, et al. 2015. Bacterial c-di-GMP affects hematopoietic stem/progenitors and their niches through STING. *Cell Rep.* 11:71–84. https://doi.org/10.1016/j.celrep.2015.02.066

Mitroulis, I., K. Ruppova, B. Wang, L.S. Chen, M. Grzybek, T. Grinenko, A. Eugster, M. Troullinaki, A. Palladini, I. Kourtzelis, et al. 2018. Modulation of myelopoiesis progenitors is an integral component of trained immunity. *Cell*. 172:147–161.e12. https://doi.org/10.1016/j.cell.2017.11.034

Mossadegh-Keller, N., S. Sarrazin, P.K. Kandalla, L. Espinosa, E.R. Stanley, S.L. Nutt, J. Moore, and M.H. Sieweke. 2013. M-CSF instructs myeloid lineage fate in single haematopoietic stem cells. *Nature*. 497:239–243. https://doi.org/10.1038/nature12026

Nebe, C.T., M. Rother, I. Brechtel, V. Costina, M. Neumaier, H. Zentgraf, U. Böcker, T.F. Meyer, and A.J. Szczepek. 2005. Detection of Chlamydophila pneumoniae in the bone marrow of two patients with unexplained chronic anaemia. *Eur. J. Haematol.* 74:77–83. https://doi.org/10.1111/j.1600-0609.2004.00353.x

Pietras, E.M. 2017. Inflammation: A key regulator of hematopoietic stem cell fate in health and disease. *Blood*. 130:1693–1698. https://doi.org/10.1182/blood-2017-06-780882

Pietras, E.M., C. Mirantes-Barbeito, S. Fong, D. Loeffler, L.V. Kovtonyuk, S. Zhang, R. Lakshminarasimhan, C.P. Chin, J.M. Techner, B. Will, et al. 2016. Chronic interleukin-1 exposure drives haematopoietic stem cells towards precocious myeloid differentiation at the expense of self-renewal. *Nat. Cell Biol.* 18:607–618. https://doi.org/10.1038/ncb3346

Pronk, C.J., O.P. Veiby, D. Bryder, and S.E.W. Jacobsen. 2011. Tumor necrosis factor restricts hematopoietic stem cell activity in mice: Involvement of two distinct receptors. *J. Exp. Med.* 208:1563–1570. https://doi.org/10.1084/jem.20110752

Reece, S.T., A. Vogelzang, J. Tornack, W. Bauer, U. Zedler, S. Schommer-Leitner, G. Stingl, F. Melchers, and S.H.E. Kaufmann. 2018. Mycobacterium tuberculosis-infected hematopoietic stem and progenitor cells unable to express inducible nitric oxide synthase propagate tuberculosis in mice. *J. Infect. Dis.* 217:1667–1671. https://doi.org/10.1093/infdis/jiy041

Salcedo, S.P., M.I. Marchesini, C. Degos, M. Terwagne, K. Von Bargen, H. Lepidi, C.K. Herrmann, T.L. Santos Lacerda, P.R.C. Imbert, P. Pierre, et al. 2013. BtpB, a novel Brucella TIR-containing effector protein with immune modulatory functions. *Front. Cell. Infect. Microbiol.* 3:28. https://doi.org/10.3389/fcimb.2013.00028

Sarrazin, S., N. Mossadegh-Keller, T. Fukao, A. Aziz, F. Mourcin, L. Vanhille, L. Kelly Modis, P. Kastner, S. Chan, E. Duprez, et al. 2009. MafB restricts M-CSF-dependent myeloid commitment divisions of hematopoietic stem cells. *Cell*. 138:300–313. https://doi.org/10.1016/j.cell.2009.04.057

Silverberg, D.S., A. Iaina, D. Wexler, and M. Blum. 2001. The pathological consequences of anaemia. *Clin. Lab. Haematol.* 23:1–6. https://doi.org/10.1046/j.1365-2257.2001.00352.x

Takizawa, H., S. Boettcher, and M.G. Manz. 2012. Demand-adapted regulation of early hematopoiesis in infection and inflammation. *Blood*. 119: 2991–3002. https://doi.org/10.1182/blood-2011-12-380113

Takizawa, H., K. Fritsch, L.V. Kovtonyuk, Y. Saito, C. Yakkala, K. Jacobs, A.K. Ahuja, M. Lopes, A. Hausmann, W.D. Hardt, et al. 2017. Pathogen-induced TLR4-TRIF innate immune signaling in hematopoietic stem cells promotes proliferation but reduces competitive fitness. *Cell Stem Cell*. 21:225–240.e5. https://doi.org/10.1016/j.stem.2017.06.013

Tatsuo, H., and Y. Yanagi. 2002. The morbillivirus receptor SLAM (CD150). *Microbiol. Immunol.* 46:135–142. https://doi.org/10.1111/j.1348-0421.2002.tb02678.x

Till, J.E., and E.A. McCulloch. 1961. A direct measurement of the radiation sensitivity of normal mouse bone marrow cells. *Radiat. Res.* 14:213–222. https://doi.org/10.2307/3570892

Weissman, I.L. 2014. Clonal origins of the hematopoietic system: The single most elegant experiment. *J. Immunol.* 192:4943–4944. https://doi.org/10.4049/jimmunol.1400902

World Health Organization. 2008. Worldwide prevalence of anaemia 1993-2005: WHO global database on anaemia. World Health Organization. https://apps.who.int/iris/handle/10665/43894 (accessed March 25, 2009).

## Supplemental material

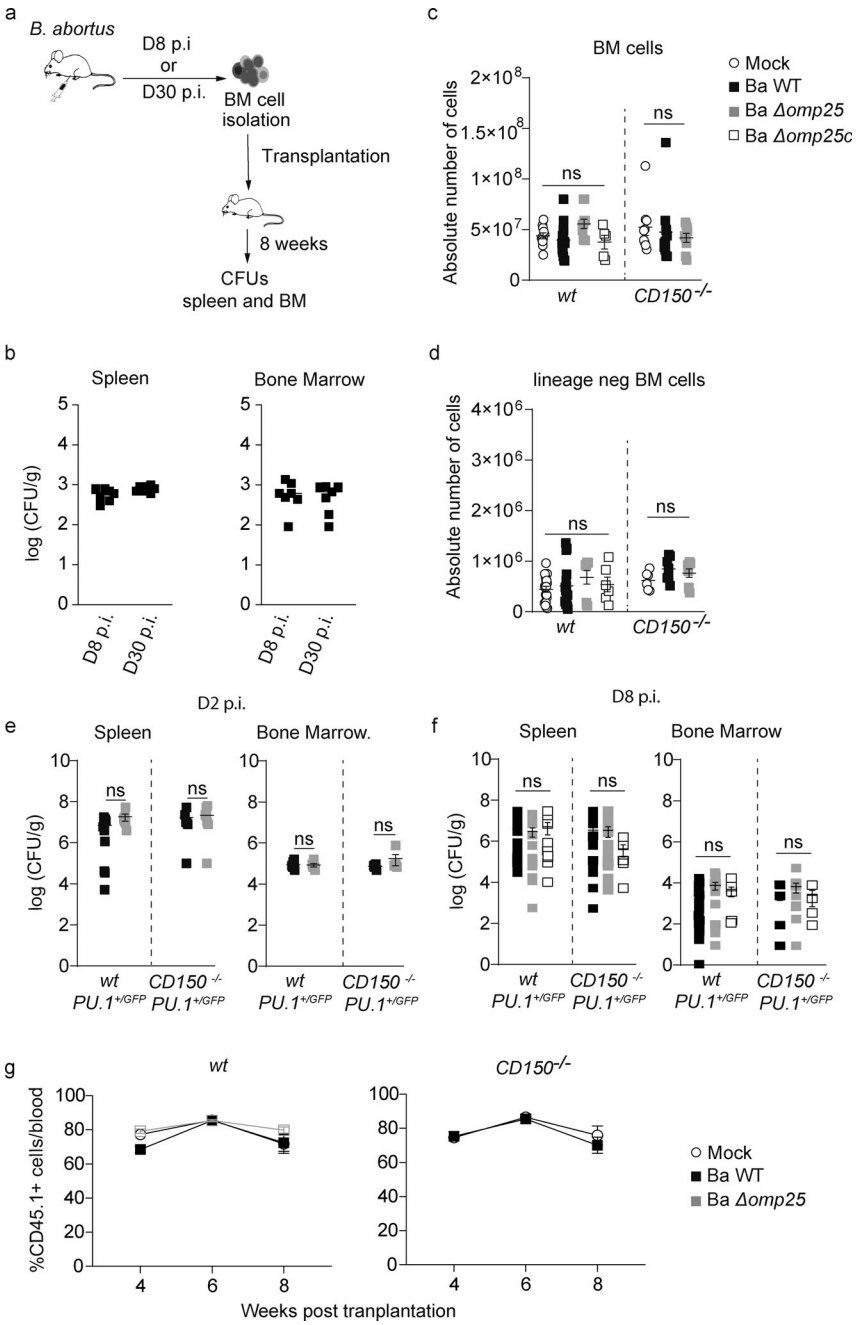


Figure S1. ***B. abortus* infection can be transferred by BM transplantation, and all *B. abortus* strains are equally virulent. (a)** Experimental scheme: Mice were intraperitoneally inoculated with 1 × $10^6$ CFU of wild-type *B. abortus*. BM cells were transplanted into previously lethally irradiated mice. 8 wk after transplantation, CFU per gram of organ was enumerated from spleens and BM. **(b)** Enumeration of CFU per gram of spleen and BM 8 wk after transplantation ($n$ = 7). **(c and d)** wt and *CD150*$^{-/-}$ mice were intraperitoneally injected with PBS or inoculated with 1 × $10^6$ CFU of *B. abortus*. 8 d later, BM cells were isolated, cells were counted (c), and then depleted for mature hematopoietic cells as shown in the Materials and methods. Lin$^-$ cells (d) were also counted for mice injected with PBS (Mock, unfilled circle) or infected *B. abortus* (Ba WT; black square), *B. abortus* Δ*omp25* (Ba Δ*omp25*; gray square) or *B. abortus* Δ*omp25* complemented with p:Omp25 (Ba Δ*omp25*c; unfilled square) mutants (the latter only for wt mice). From left to right: for BM, $n$ = 11, 14, 8, 5, 9, 11, 9; and for lin$^-$ BM, $n$ = 18, 16, 8, 6, 6, 7, 9. Data were obtained from distinct samples from five independent experiments. **(e and f)** CFU counts per gram of organ at day 2 (e) and day 8 (f) after infection for spleen and BM of mice infected with Ba WT (black square), Ba Δ*omp25* (gray square) or Ba Δ*omp25*c (unfilled square). For day 2 (D2) spleen, $n$ = 9, 6, 8, 8; for day 2 (D2) BM, $n$ = 6, 6, 7, 7; for day 8 (D8) spleen, $n$ = 19, 15, 9, 15, 23, 6; for day 8 (D8) BM, $n$ = 5, 11, 4. Data were obtained from distinct samples from four independent experiments (a–d), each with at least three animals. Mean ± SEM is represented by a horizontal bar. Significant differences from mock are shown. Absence of P value or ns, non-significant. Since data did not follow normal distribution, P values were generated using Kruskal–Wallis followed by Dunn's test. **(g)** Contribution of HSC from wt CD45.1 (left panel) and *CD150*$^{-/-}$ CD45.1 (right panel) mice incubated for 30 min ex vivo with Ba WT (black square) or Ba Δomp25 (gray square) or non-infected (Mock, unfilled circle) as described in Fig. 3 e, to blood chimerism in CD45.2 recipients, at 4, 6, and 8 wk after transplantation (from left to right: for WT, $n$ = 12, 13, 10, 10, 9, 9, 12, 8, 8; and for CD150$^{-/-}$, $n$ = 9, 4, 14, 8, 11, 7). Data were obtained from repetitive sampling from two independent experiments. Mean ± SEM is represented by horizontal bar. Absence of P value, non-significant. Since data did not follow normal distribution, P values were generated using Kruskal–Wallis followed by Dunn's test.

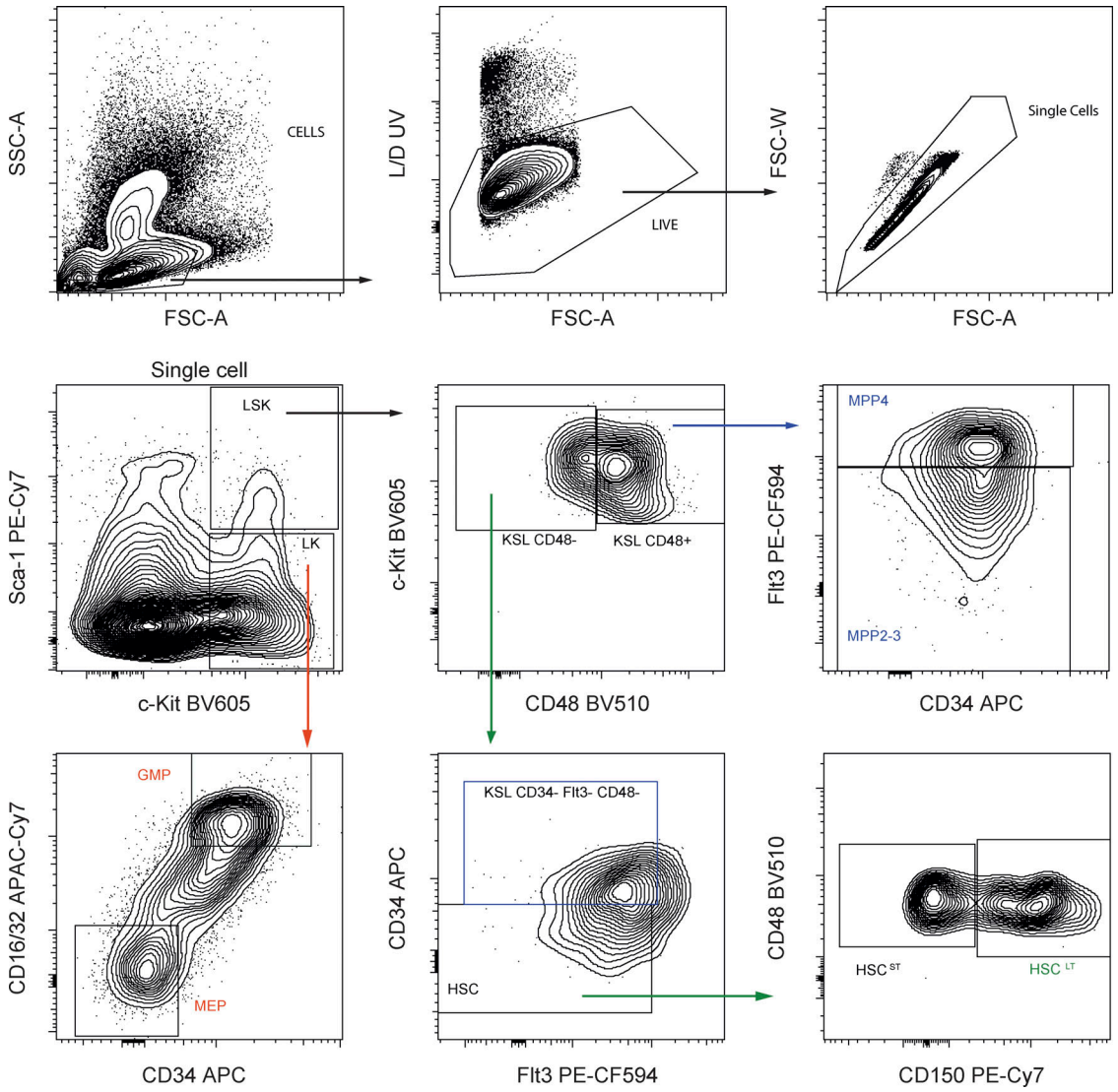


Figure S2. **FACS gating for analysis of HSC and progenitors from lineage negative fraction of BM.** First, cells were gated based on SSC/FSC, and then single cells were selected. Viable cells were gated using UV Fixable Blue Dead stain. Described population are: LSK (lin$^-$, Sca$^+$, cKit$^+$), LT-HSC (lin$^-$, Sca$^+$, cKit$^+$, CD48$^-$, CD135$^-$, CD34$^-$, CD150$^+$), MPP2-3 (lin$^-$, Sca$^+$, cKit$^+$, CD48$^+$, CD135$^-$), MPP4 (lin$^-$, Sca$^+$, cKit$^+$, CD48$^+$, CD135$^+$), GMP (lin$^-$, Sca$^-$, cKit$^+$, CD34$^+$, CD16/32$^+$), and MEP (lin$^-$, Sca$^-$, cKit$^+$, CD34$^-$, CD16/32$^-$).

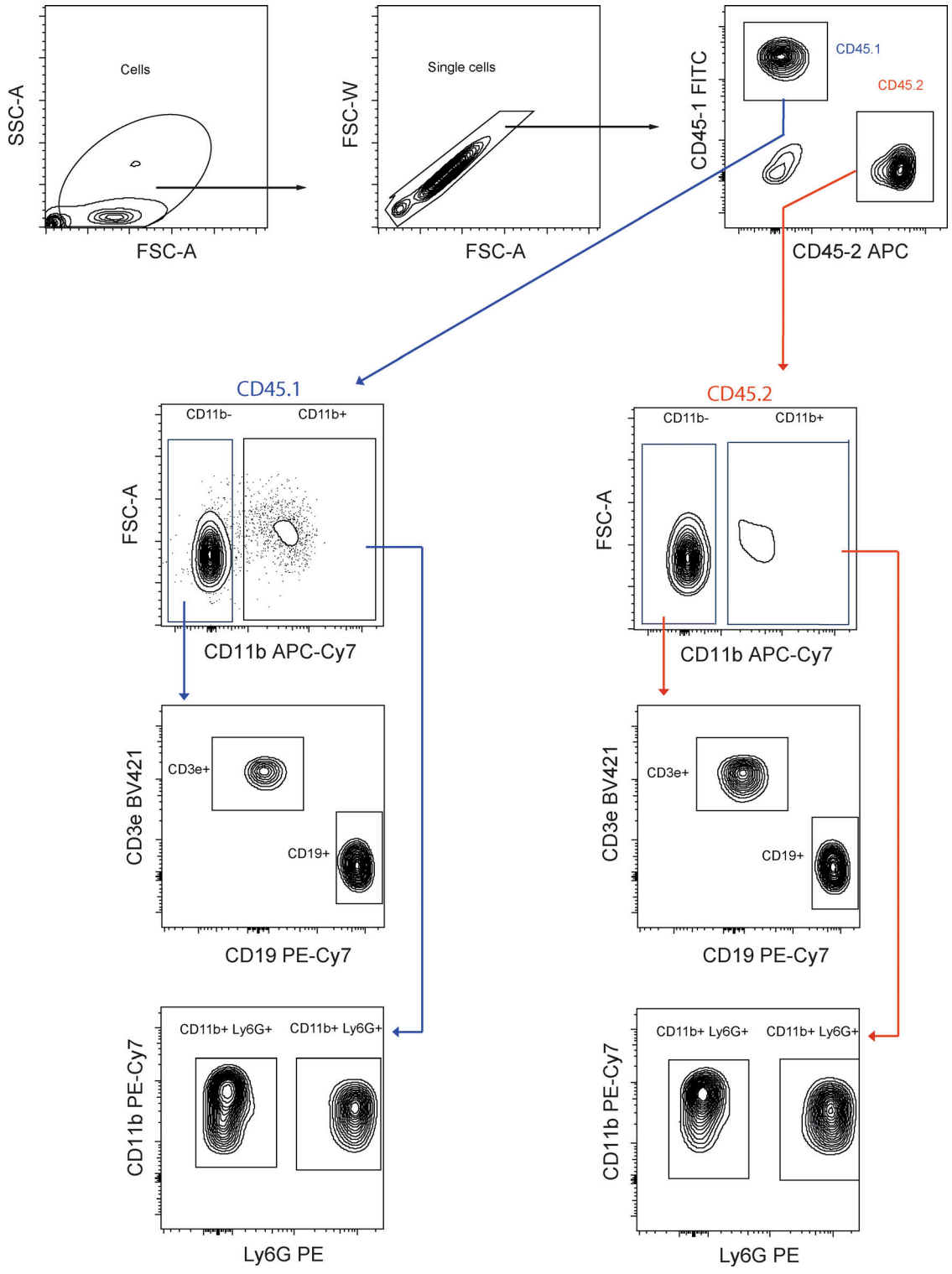


Figure S3. **FACS gating for blood analysis from chimeric mice.** Complete FACS gating for blood lineage output from chimeric mice. First, cells were gated based on SSC/FSC, and then single cells were selected. *CD150*$^{-/-}$ and wt cells were separated by gating on, respectively, CD45.1- and CD45.2-positive cells. In each, lymphoid cells were isolated by gating on CD11b-negative cells; then, B cells were CD19-positive cells, and T cells were CD3ε-positive cells. In Cd11b-positive cells, granulocytes and monocytes are distinguished by gating onto, respectively, Ly6G-positive and -negative cells.